

Electronic Supplementary Information for

Framework nucleic acid programmed combinatorial delivery nanocarriers for parallel and multiplexed analysis

Yinghui Feng,^a Qi Liu,^{*,a} Miao Chen,^{a,b} Xinyi Zhao,^a Lumin Wang,^a Longfei Liu,^c and Xiaoqing Chen^{*,a}

^a College of Chemistry and Chemical Engineering, the Hunan Provincial Key Laboratory of Water Environment and Agriculture Product Safety, Central South University, Changsha 410083, Hunan, China.

^b College of Life Science, Central South University, Changsha 410083, Hunan, China.

^c Department of Urology, Xiangya Hospital, Central South University, Changsha 410008, Hunan, China.

E-mail address: iliuqi@csu.edu.cn, xqchen@csu.edu.cn.

EXPERIMENTAL SECTION

Materials.

Tris(hydroxymethyl) aminomethane (Tris), sodium chloride (NaCl), potassium chloride (KCl), magnesium chloride (MgCl₂), Ethylene Diamine Tetraacetic Acid (EDTA), and boric acid(H₃BO₃) were purchased from China National Pharmaceutical Group Corporation (Shanghai, PRC). All aqueous solutions were prepared using ultrapure water ($\geq 18\text{ M}\Omega$, Milli-Q water purification system, Millipore). All oligonucleotide sequences shown in Table S1 were synthesized and modified by Sangon Biotechnology Co., Ltd. (Shanghai, PRC).

Cell Culture.

Human breast cancer cell line MCF-7, human lung adenocarcinoma cell line A549, human prostate cancer cell line PC-3, and human normal hepatic cell line QSG-7701 were obtained from Beyotime Biotechnology (Shanghai, PRC). Cell Counting Kit-8(CCK-8) and cell culture products were purchased from GIBCO (USA). MCF-7, PC-3, and QSG-7701 were cultured in Roswell Park Memorial Institute 1640 with 10% fetal bovine serum, while A549 was cultured in Dulbecco's Modified Eagle medium with high glucose with 10% fetal bovine serum (Gibco FBS, South America origin, Thermo). Those cell lines were cultured at 5% CO₂ atmosphere under 37 °C.

Assembly of TNCs.

Mono-TNCs with different capture probe T1, T2 and T3 were synthesized by mixing equimolar quantities (1 μM) of oligonucleotides (Table S1) in TM buffer (20 mM Tris, 50mM MgCl₂, pH 8.0),

then heated to 95 °C for 10 min, and rapidly cooled to 4 °C within 30 s by using PTC-200 (MJ. Research Inc., SA).

“Bottom-up” construction of FNAs including di-TNC and tri-TNC was realized by mixing DNA scaffold and DNA sequences in equimolar amounts (Table S2), and incubating under 37 °C for 120 min in PB buffer (20 mM Tris, 1 M NaCl, 20 mM MgCl₂, pH 8.0) respectively. All FNA scaffolds were characterized by 2% agarose gel electrophoresis (AGE, contain 0.01% GelRed) within 1× TBE buffer (40 mM Tris, 25 mM H₃BO₃, 1 mM EDTA), run at 100 V for 40 mins and analyzed on a chemiluminescence imaging system (G:Box Chemi-XL).

Purification and characterization of TNCs.

An Agilent 1260 HPLC system (equipped with a 1260 infinity quaternary pump, a 1260infinity variable wavelength detector, and an infinity 1260 analytical scale fraction collector, Agilent, USA) and a size exclusion chromatography (SEC) column (Phenomenex BioSec-SEC-4000, 300*7.8 mm) were used for HPLC purification of TNCs, all chromatograms were recorded at 260 nm. The SEC mobile phase was composed of 30 mM of Tris-HCl and 450 mM of NaCl, pH 7.4. 100–500 µL of as prepared TNCs were loaded and purified at a flow rate of 1.0 mL/min with isocratic elution. Peak fractions collected from SEC were concentrated at 5000 g for 5-20 min using Amicon Ultra-0.5 mL centrifugal filters (MWCO 100 kDa), and the solvent was displaced by TM buffer, then the concentration of each sampler was quantified with a UV-vis absorption spectrophotometer (Hitachi U-3010, Japan).

The purified TNCs were characterized by atomic force microscope (AFM, Bruker, USA). Freshly cleaved mica surface was modified with 0.5% APTES for 2 min, and washed off by ultrapure water, then dried by compressed air. DNA nanostructures, diluted to 10 nM in TM buffer in 10 µL, were spotted onto mica surface and incubated for 5 min to allow the sample to absorb onto the substrate. After that, additional TM buffer was added to a total volume of 40 µL, and the sample was scanned using an SNL-10 (Veeco Inc., USA) with supersharp tips of 2-3 nm radius.

miRNA Fluorescence detection *in vitro*.

Detection of target miRNA was done by measuring the fluorescence signals of fluorophores using synchronous scanning fluorescence spectroscopy (Perkin Elmer LS-55, UK). The wavelength intervals between the maximum excitation and emission wavelengths of Alex Fluor 488, ROX and Cy5 were set at 25 nm, 20 nm and 20 nm, respectively. In order to realize the simultaneous detection

of the three fluorophores, the fixed wavelength difference ($\Delta\lambda$) of synchronous scanning fluorescence spectroscopy was set as 22 nm. The human serum samples were obtained from The Third Xiangya Hospital of Central South University, and this study was approved by the Medical Ethics Committee of The Third Xiangya Hospital of Central South University.

CCK-8 Assay.

MCF-7, PC-3, A549 and QSG-7701 cells (5×10^3 cells/well) were seeded in 96-well microtiter plates to a total volume of 100 μ L per well and were incubated at 37 °C in a 5% CO₂ incubator for 24 h, respectively. Then the original medium was removed, and the MCF-7, PC-3, A549 and QSG-7701 cells were incubated with fresh medium containing DNA nanoprobe for 2, 6, 12, and 24 h. Ultimately, the cells were washed with 1 \times PBS for three times and 10 μ L of CCK-8 solutions were added into each well. After being incubated for 2 h, the absorbance of the solution was measured at 450 nm with a THERMO FISHER Multiskan FC (USA).

Cell fluorescence detection.

For flow cytometric analysis, fluorescence was collected by BD Accuri C6 plus Flow Cytometer. Also, the expression levels of miRNA-141 (Alexa488), miRNA-21 (ROX) and miRNA-155 (Cy5) in cells were detected by using High Content Analysis System Operetta CLSTM at the excitation/emission wavelengths of 460-490/500-550 nm for Alaxe 488, 530-560/570-620 nm for ROX, and 615-645/655-760 nm for Cy5.

Table S1. DNA sequences used in our experiments

| DNA | DNA sequence (5'-3') |
|------------|--|
| Linker-DNA | <u>CCT GAG GTC AGG AGT TCG AGA CCA GCC TGG C</u> CA ACA TGG TGA AAC CCC GTC TCT ACT AAA AAT ACA AAA ATT A GC CGG GCG TGG TGG CGC GCG CCT GTA ATC CCA GCT ACT CGG G |
| A37.1 | CCC TGT ACT GGC TAG GAA TTC ACG TTT TAA TCT GGG C TTT GG GTT AAG AAA CTC CCC G CG |
| A37.2-T1 | CTG GAG GC GCA TCA CCG TTT GCG TAT GTG TTC TGT GCG GCC TGC CGT CCC GTG TGG G <u>G C CAG GCT GGT CTC GAA CTC CTG ACC TCA GG</u> |
| A37.2-T2 | CTG GAG GC GCA TCA CCG TTT GCG TAT GTG TTC TGT GCG GCC TGC CGT CCC GTG TGG G <u>TA ATT TTT GTA TTT TTA GTA GAG ACG GGG TTT</u> <u>CAC CAT GTT G</u> |
| A37.2-T3 | CTG GAG GC GCA TCA CCG TTT GCG TAT GTG TTC TGT GCG GCC TGC CGT CCC GTG TGG G <u>CC CGA GTA GCT GGG ATT ACA GGC GCG CGC CAC</u> <u>CAC GCC CGG C</u> |

| | |
|----------------|---|
| B37.1-BHQ1 | CGG TGA TGC GCC TCC AGC GCG GGG AGT TTC TTA ACC C TT TCC GAC TTA CAA GAG CCG GG BHQ1 |
| B37.1-BHQ2 | CGG TGA TGC GCC TCC AGC GCG GGG AGT TTC TTA ACC C TT TCC GAC TTA CAA GAG CCG GG BHQ2 |
| B37.1-BHQ3 | CGG TGA TGC GCC TCC AGC GCG GGG AGT TTC TTA ACC C TT TCC GAC TTA CAA GAG CCG GG BHQ3 |
| B37.1-W30 | CGG TGA TGC GCC TCC AGC GCG GGG AGT TTC TTA ACC C TT TCC GAC TTA CAA GAG CCG GG TACGAGTGGAGAATCCTGAATGCGACTGTT |
| M30-50A | AA AAAAAAACAGTCGCATTCAGGATTCTCCACTCGTA |
| B37.2-Alexa488 | Alexa488 CGAGA CTC AGG TGG TGC CTT TGG CAT TCG ACC AGG AGA TAT CGC GTT CAG CTA TGC CC |
| B37.2-ROX | ROX CGAGA CTC AGG TGG TGC CTT TGG CAT TCG ACC AGG AGA TAT CGC GTT CAG CTA TGC CC |
| B37.2-CY5 | GY5 CGAGA CTC AGG TGG TGC CTT TGG CAT TCG ACC AGG AGA TAT CGC GTT CAG CTA TGC CC |
| C37.1 | CCC ATG AGA ATA ATA CCG CCG ATT TAC GTC AGT CCG GTT TCC CAC ACG GGA CGG CAG GC |
| C37.2 | CGC ACA GAA CAC ATA CGC TTT GGG CAT AGC TGA ACG CGA TAT CTC CTG GTC GAA TGC C |
| D37.1 | GCC CAG ATT AAA ACG TGA ATT CCT AGC CAG TAC AGG GTT TCC GGA CTG ACG TAA ATC GG |
| D37.2 | CGG TAT TAT TCT CAT GGG TTT GGC ACC ACC TGA GTC TCG CCC GGC TCT TGT AAG TCG G |
| D37.2-141 | CGG TAT TAT TCT CAT GGG TTT GGC ACC ACC TGA GTC TCG TAA CAC TG C CAT CTT TAC CAG ACA GTG TTA CCC GGC TCT TGT AAG TCG G |
| D37.2-21 | CGG TAT TAT TCT CAT GGG TTT GGC ACC ACC TGA GTC TCG TAG CTT AT T TCAA CAT CAG TCT GAT AAG CTA CCC GGC TCT TGT AAG TCG G |
| D37.2-155 | CGG TAT TAT TCT CAT GGG TTT GGC ACC ACC TGA GTC TCG TTA ATG CT T ACC CCT ATC ACG ATT AGC ATT AA CCC GGC TCT TGT AAG TCG G |
| T1-Comp. | TCG AGA CCA GCC TGG |
| T3-Comp2. | GCC GGG CGT GGT GGC GCG CGC C |
| 10T-T3 | TTT TTT TTT TCC CGA GTA GCT GGG ATT ACA GGC GCG CGC CAC CAC GCC CGG C |
| miRNA-141 | UAA CAC UGU CUG GUA AAG AUG G |
| miRNA-21 | UAG CUU AUC AGA CUG AUG UUG A |
| miRNA-155 | UUA AUG CUA AUC GUG AUA GGG GU |
| Apt-ATP | <u>TGG GGGAGTATTGCGGAGGAAGGT</u> |

| | |
|-----------|---|
| Apt-Thr | AGTCCGTGGTAGGGCAGGTTGGGGT <u>GACTATCAAG</u> |
| D37.2-ATP | CGG TAT TAT TCT CAT GGG TTT GGC ACC ACC TGA GTC TCG <u>ACCTGGGAATACTCCCCAGGT</u> CCC GGC TCT TGT AAG TCG G |
| D37.2-Thr | CGG TAT TAT TCT CAT GGG TTT GGC ACC ACC TGA GTC TCG <u>CTTGATAGTCACCATCAAG</u> CCC GGC TCT TGT AAG TCG G |

Table S2. DNA sequences combinations for scaffolds construction

| DNA structure | DNA sequence contained |
|---------------|---|
| TNC-141 | A37.1, A37.2-T1, B37.1, B37.2, C37.1, C37.2, D37.1, D37.2-141, T1-Comp. |
| TNC-21 | A37.1, A37.2-T2, B37.1, B37.2, C37.1, C37.2, D37.1, D37.2-21 |
| TNC-155 | A37.1, A37.2-T3, B37.1, B37.2, C37.1, C37.2, D37.1, D37.2-155, T3-Comp2. |
| TNC-AuNPs1 | A37.1, A37.2-T1, B37.1-W30, B37.2, C37.1, C37.2, D37.1, D37.2, T1-Comp. |
| TNC-AuNPs2 | A37.1, A37.2-T2, B37.1-W30, B37.2, C37.1, C37.2, D37.1, D37.2 |
| TNC-AuNPs3 | A37.1, A37.2-T3, B37.1-W30, B37.2, C37.1, C37.2, D37.1, D37.2, T3-Comp2. |
| TNC-ATP | A37.1, A37.2-T1, B37.1, B37.2, C37.1, C37.2, D37.1, D37.2-ATP, T1-Comp. |
| TNC-Thr | A37.1, A37.2-T3, B37.1, B37.2, C37.1, C37.2, D37.1, D37.2-Thr, Apt-Thr T3-Comp2. |
| di-TNC | TNC-141, TNC-21, 10T-T3, T-DNA/ TNC-AuNPs1, TNC-AuNPs2, 10T-T3, T-DNA |
| tri-TNC | TNC-141, TNC-21, TNC-155, T-DNA/ TNC-AuNPs1, TNC-AuNPs2, TNC-AuNPs3, T-DNA/ TNC-ATP, TNC-21, TNC-Thr, T-DNA |

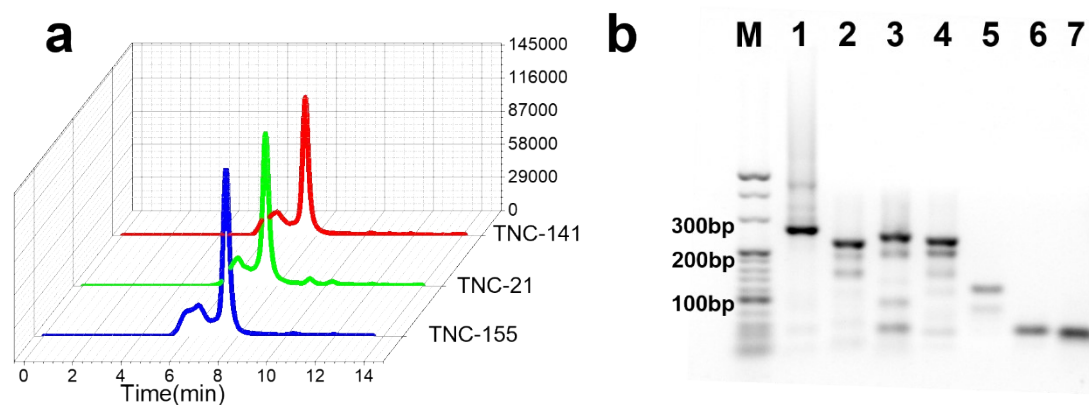


Fig. S1 (a) HPLC chromatograms of mono-TNC (TNC-141, TNC-21, TNC-155). (b) The synthesis of TNC-141 (mono- TNC) was characterized by 2% AGE. Lane 1 is A37.1+A37.2-T1+B37.1-BHQ1+B37.2-ALEXA488+C37.1+C37.2+D37.1+ D37.2-141+T1-comp.; Lane 2 is B37.1-BHQ1+B37.2-ALEXA488+C37.1+C37.2+D37.1+ D37.2-141; Lane 3 is A37.1+A37.2-T1+C37.1+C37.2+ D37.1+D37.2-141+T1-comp.; Lane 4 is A37.1 +A37.2-T1+B37.1-BHQ1+B37.2-ALEXA488+C37.1+C37.2 +T1-comp.; Lane 5 is B37.1-BHQ1+ B37.2-ALEXA488+D37.2-141; Lane 6 is A37.2-T1+T1-Comp.; Lane 7 is D37.2-141; M is a 20 bp ladder.

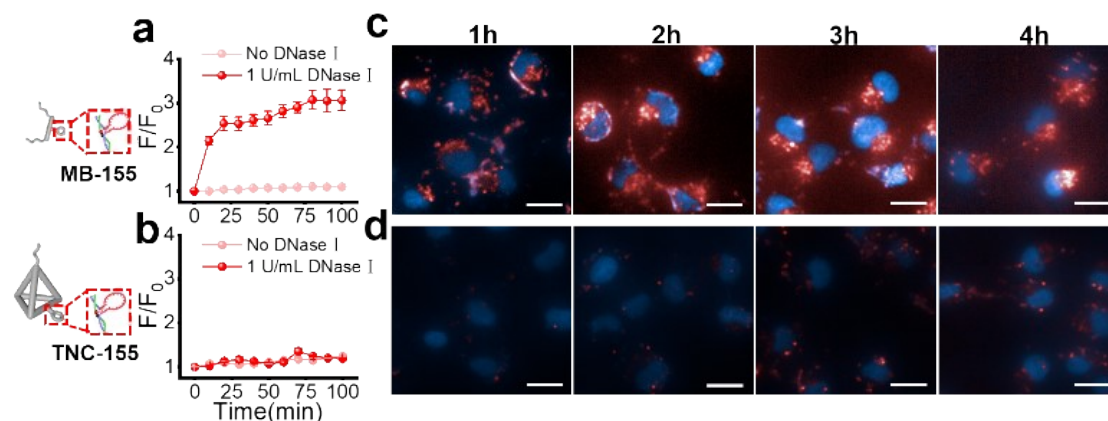


Fig. S2 Comparisons of the stability against protease digestion for (a) free hairpin (MB-155, 50 nM) and (b) carbone beacon (TNC-155, 50 nM) which were incubated with Dnase I (1 U/mL). Fluorescence images of miRNA-155 in MCF-7 cells incubated with (c) free hairpin (MB-155) and (d) carbone beacon (TNC-155), respectively. Scale bar: 20 μ m.

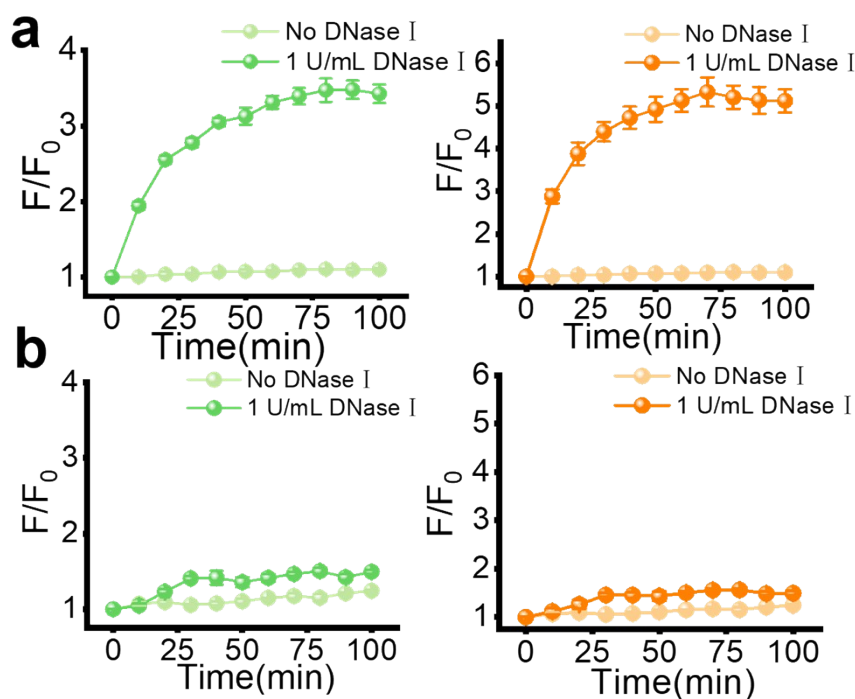


Fig. S3 Comparisons of the stability against protease digestion for (a) free hairpin (MB-141 and

MB-21, 50 nM) and (b) carbone beacon (TNC-141 and TNC-21, 50 nM) which were incubated with Dnase I (1 U/mL), (From left to right, Alexa488, ROX).

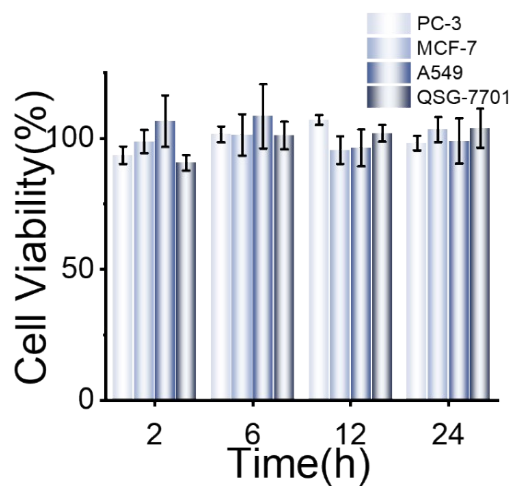


Fig. S4 Cell viability assay (CCK-8) results for PC-3, MCF-7, A549, and QSG-0771 cell lines treated with the nanocarrier mono-TNC (100 nM) for 2, 6, 12 and 24 h at 37°C.

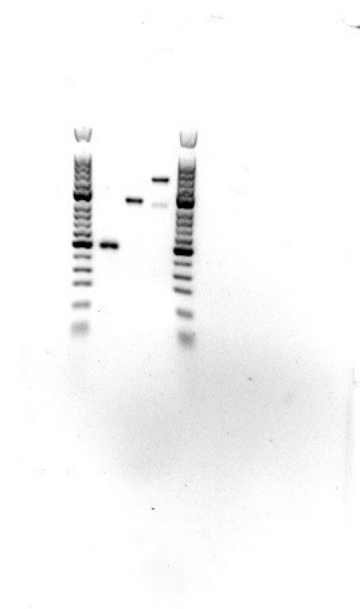


Fig. S5 Uncropped image of the AGE of tri-TNC.

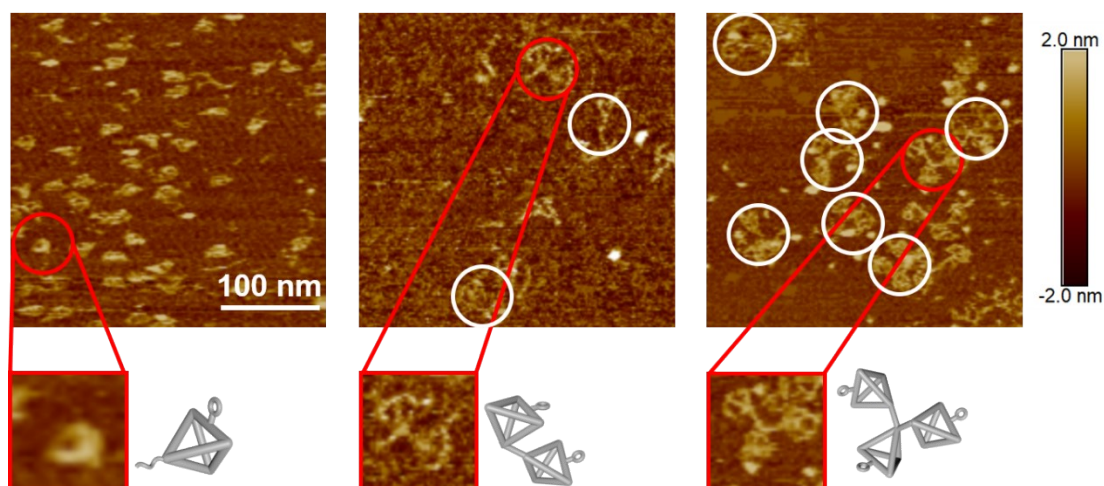


Fig. S6 The broad field AFM images of mono-, di- and tri-TNC (from left to right).

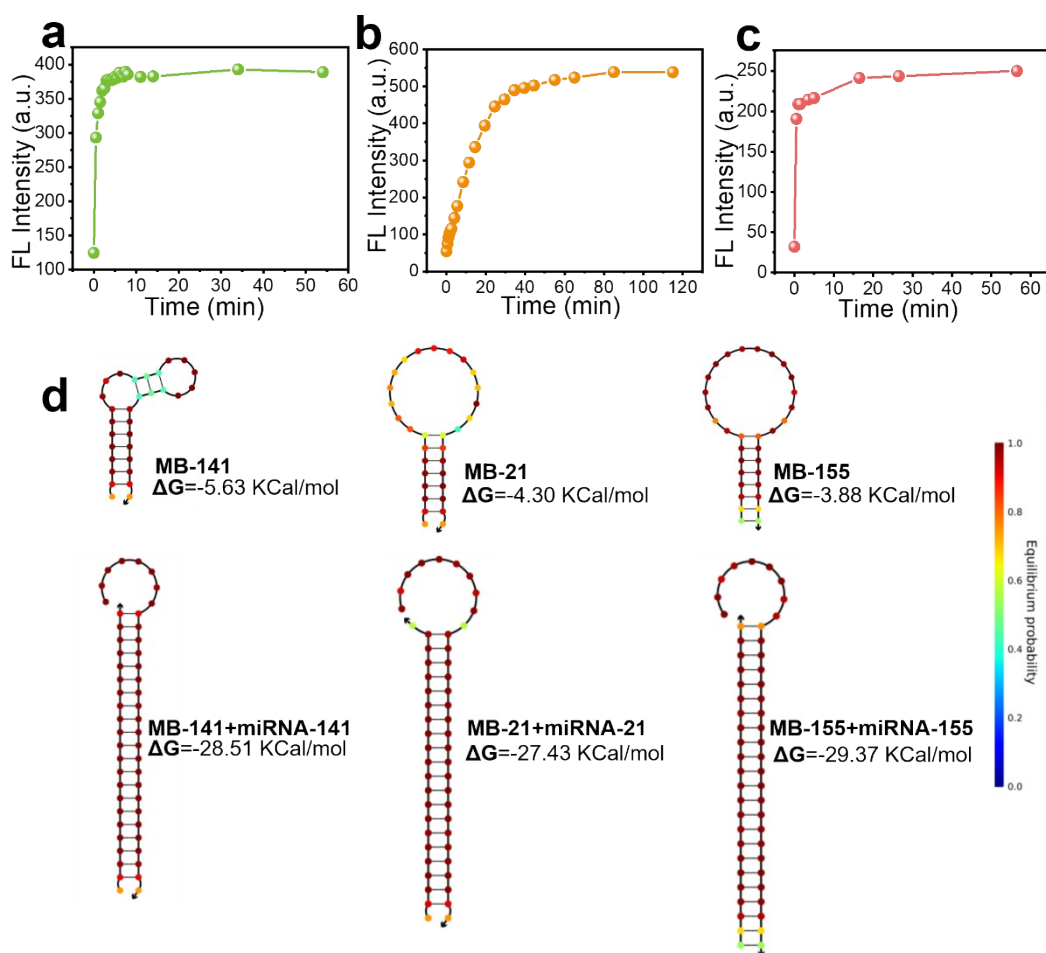


Fig. S7 The fluorescence intensities of Alexa488, ROX and Cy5 were monitored after adding three miRNA targets, respectively. **(a-b)** Alexa488 and Cy5 the fluorescence intensities restored rapidly within 1 min after adding the target. **(c)** The fluorescence intensity of ROX restored slower than that of Alexa488 and Cy5 within 80 min. As analyzed *via* NUPACK **(d)**, the different kinetics of Alexa488, ROX and Cy5 might be attributed to that, compared with MB-141 and MB-155, MB-21

had a higher free energy and a lower stability after binding to the target. Even so, the obtained stable signal outputs in given conditions provided the tri-TNC an excellent foundation for the follow-up applications.

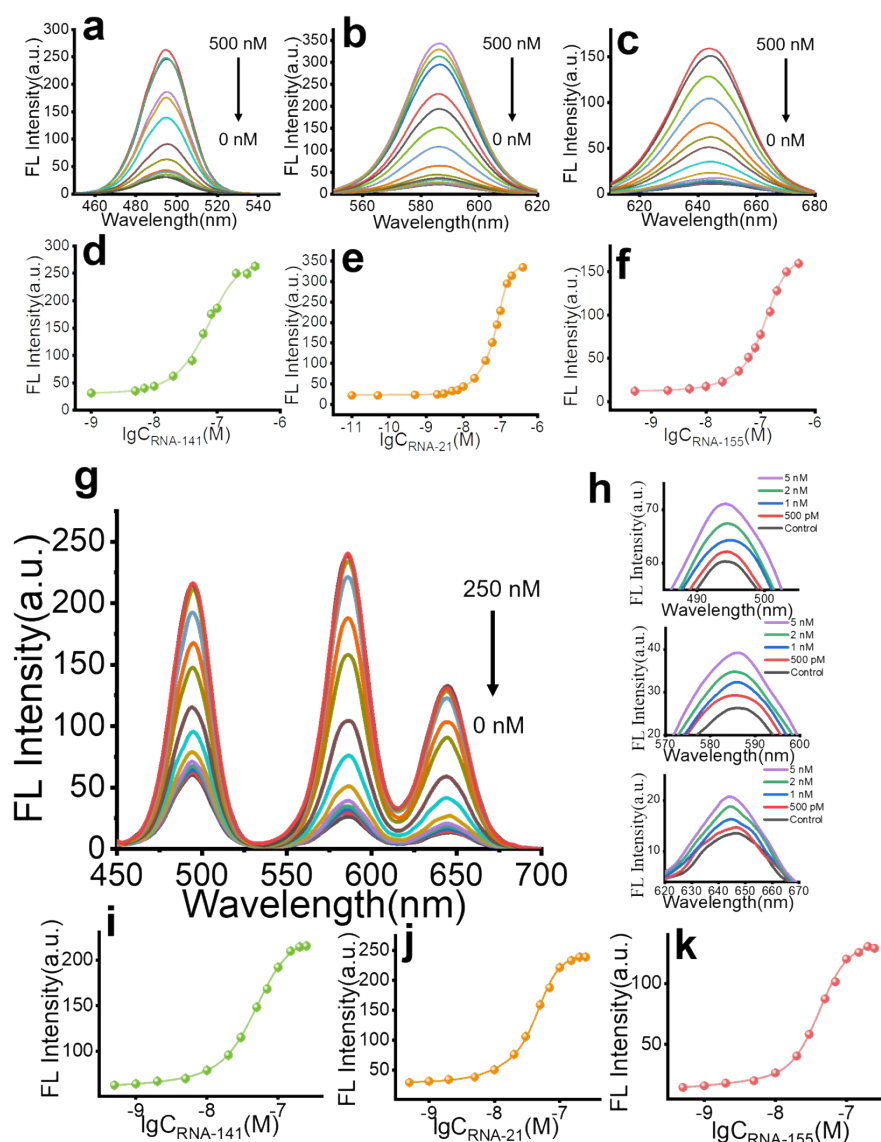


Fig. S8 Detection performances of the tri-TNC for three miRNAs in homogeneous solutions (PBS). Fluorescence spectral response of tri-TNC structure (50 nM) to varied targets **(a)** miRNA-141, **(b)** miRNA-21 and **(c)** miRNA-155 at different concentrations in a homogeneous solution, respectively. **(d-f)** show the correlation between the fluorescence intensity and the corresponding concentration of the target, respectively. **(g)** Fluorescent spectra of tri-TNC (50 nM) structure treated with three miRNA targets (0-250 nM). **(h)** Detail image show the corresponding fluorescent spectra of the concentrations of 500pM, 1nM, 2nM, 3nM. **(i-k)** show the correlation between the corresponding concentration and fluorescence intensity, respectively. Error bars represent the standard deviation from three independent assays.

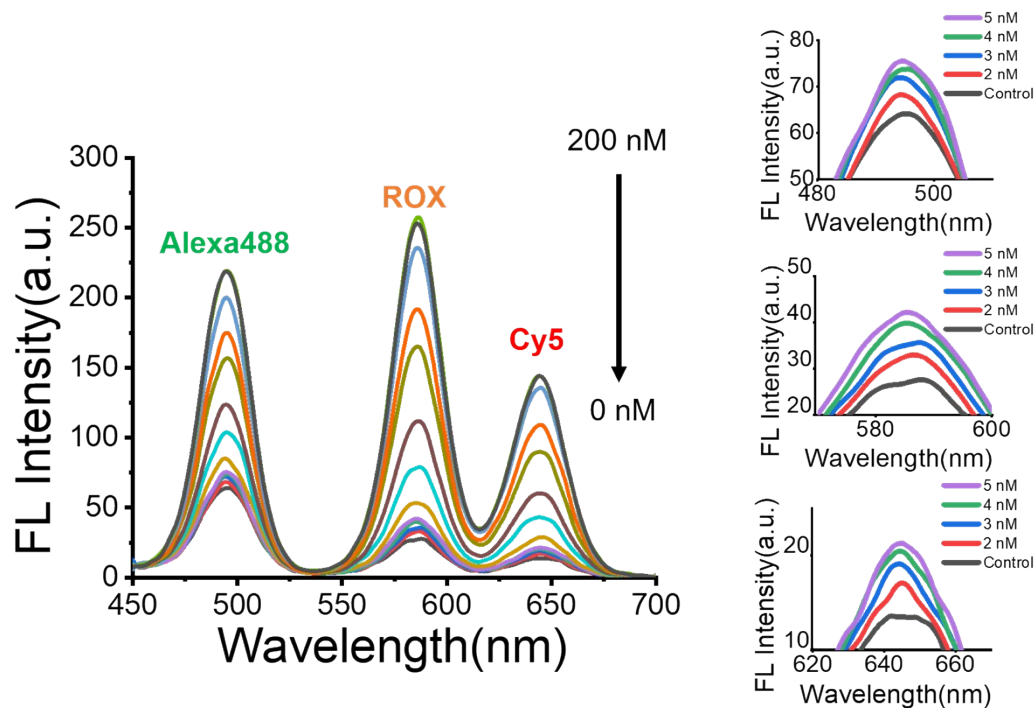


Fig. S9 Detection performance of the tri-TNC for three miRNAs in 10-fold diluted serum samples. Fluorescent spectra of a mixed solution consisting of three miRNA targets (0-200 nM) and tri-TNC (50 nM); insert views on the right show the corresponding fluorescent spectra for the concentrations of 2 nM, 3 nM, 4 nM and 5 nM.

Table S3. The recoveries of miRNA-141, miRNA-21 and miRNA-155 in 10-fold diluted serum samples from prostate cancer patients.

| sample no. | miRNA-141 | | | | miRNA-21 | | | | miRNA-155 | | | |
|------------|------------|------------|--------------|-------------------|------------|------------|--------------|-------------------|------------|------------|--------------|-------------------|
| | added (nM) | found (nM) | recovery (%) | RSD (% $n=3$) | added (nM) | found (nM) | recovery (%) | RSD (% $n=3$) | added (nM) | found (nM) | recovery (%) | RSD (% $n=3$) |
| 1 | 5 | 5.14 | 102.73 | 1.53 | 5 | 5.05 | 101.00 | 2.41 | 5 | 4.97 | 99.33 | 3.96 |
| 2 | 10 | 10.03 | 100.31 | 0.80 | 10 | 10.13 | 101.27 | 1.17 | 10 | 9.99 | 99.88 | 1.02 |
| 3 | 5 | 4.98 | 99.45 | 1.02 | 5 | 4.98 | 99.61 | 0.75 | 5 | 5.00 | 100.10 | 3.48 |
| 4 | 10 | 9.94 | 99.37 | 0.84 | 10 | 10.04 | 100.43 | 1.15 | 10 | 10.11 | 101.06 | 3.51 |
| 5 | 50 | 50.19 | 100.38 | 0.92 | 50 | 49.97 | 99.95 | 0.07 | 50 | 49.08 | 98.15 | 1.03 |

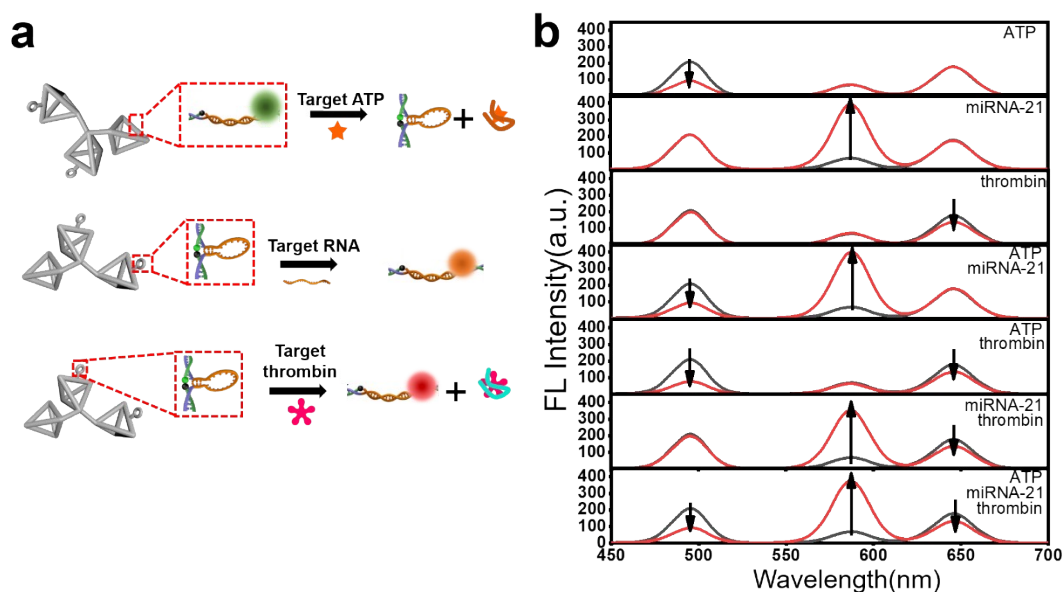


Fig. S10 (a) Schematic illustration of the proposed nanocarriers enabled multiplexed analysis of ATP, miRNA-21, and thrombin; (b) A mixed solution consisting of different components of targets was treated with tri-TNC loaded three molecular beacons for ATP, miRNA-21, and thrombin (200 nM).

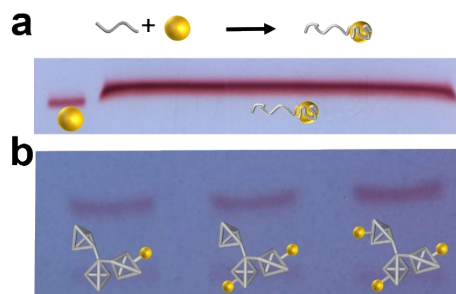


Fig. S11 (a) Schematic and AGE image of the AuNPs functionalized with the M30-50A via poly-adenine-mediation; (b) AGE image of the valence-controlled assemblies of AuNPs-tri-TNC.

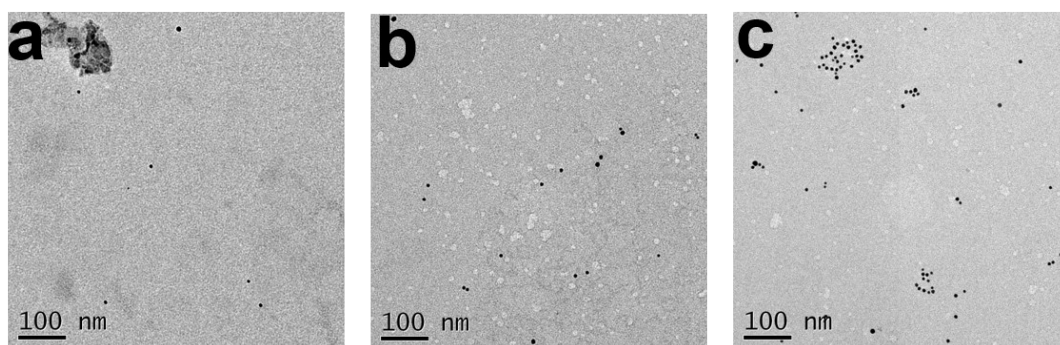


Fig. S12 The broad field TEM images of the valence-controlled assemblies of AuNPs from 1 to 3

3(a to c) respectively.

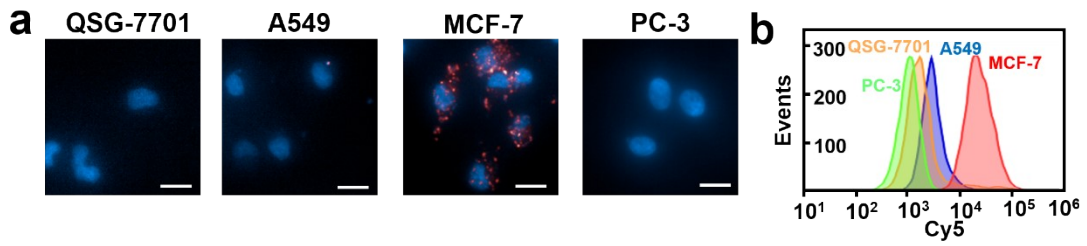


Fig. S13 (a) Fluorescence images of miRNA-155 in four cell lines (MCF-7, PC-3, A549 and QSG-7701) incubated with tri-TNC (100 nM). **(b)** Detection of miRNA-155 expression levels in different cell lines *via* flow cytometry. Scale bar: 20 μ m.

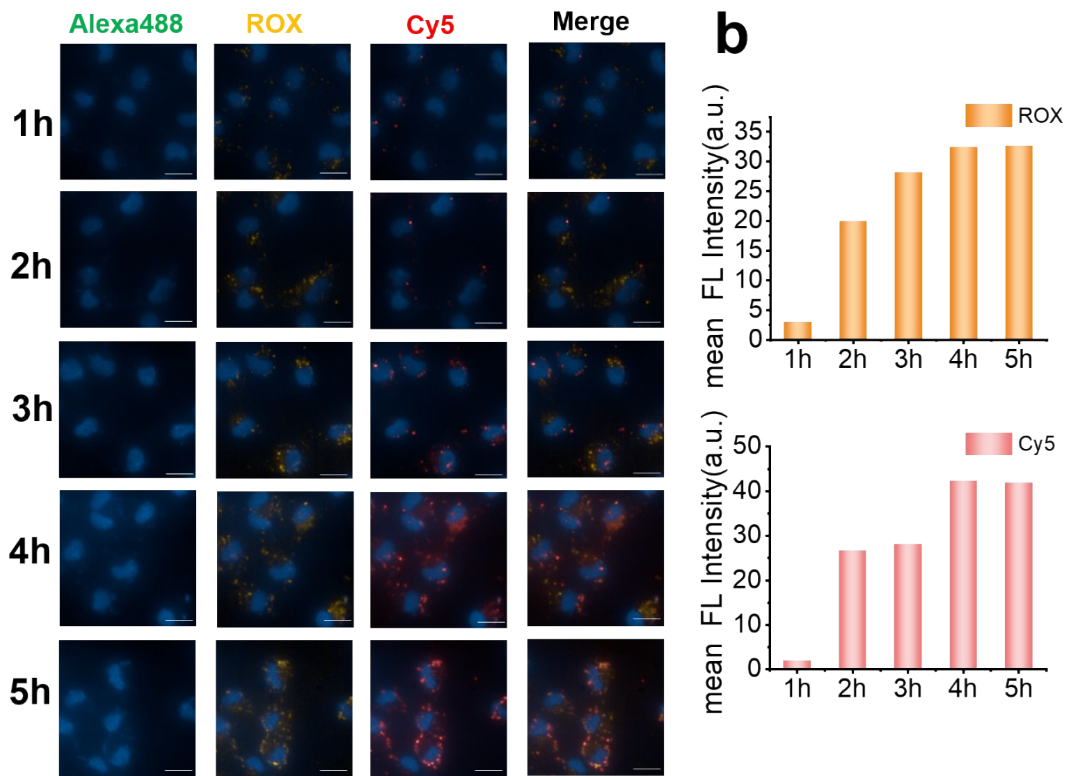


Fig. S14 (a) Fluorescence images of MCF-7 cells after being incubated with tri-TNC (100 nM) for different period times (1, 2, 3, 4 and 5h) and **(b)** the corresponding column charts of fluorescence intensity. Scale bar: 20 μ m.

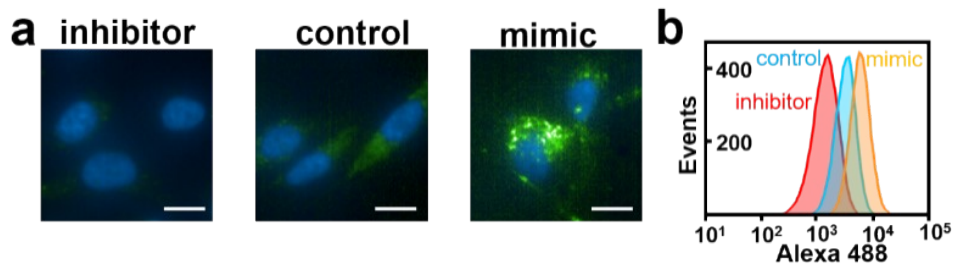


Fig. S15 (a) Fluorescence images of PC-3 cells treated with a miRNA-141 mimic and inhibitor, and the non-treated PC-3 cells were served as a control. **(b)** Detection of Alexa 488 fluorescence levels in PC-3 cells via flow cytometry. Scale bar: 20 μm .